INTERPRETATION OF THE GNEVYSHEV-OHL EFFECT AND MODULATION OF GALACTIC COSMIC RAYS BY SOLAR ACTIVITY

© 2025 I. Yu. Grigorieva[a, *], V. A. Ozheredov[b], A. B. Struminsky[b, **]

[a]*Main (Pulkovo) Astronomical Observatory, Saint-Petersburg, Russia*

[b]*Space Research Institute, Moscow, Russia*

**e-mail: irina.2014.irina@mail.ru*

***e-mail: astrum@cosmos.ru*

Received March 17, 2025

Revised April 27, 2025

Accepted June 17, 2025

Abstract. The available data for complete magnetic cycles from the 18th to the current moment of the 25th cycle are studied, relative to the maxima of galactic cosmic rays (GCR) in even cycles (in the 18th, the minimum of the SSN cycle is taken as 0): the sunspot number (SSN), the polar magnetic field (Bpol) and the Moscow neutron monitor (NM MOSC). The asymmetry of even and odd 11-year solar activity (SA) cycles in a complete 22-year magnetic cycle (visible in Bpol, GCR and SSN) corresponds to the Gnevyshev-Ohl rule (GOR). It is caused by the appearance of sunspot cycles in the decay phase of odd, which provide an additional non-zero magnetic flux necessary to form the maximum dipole magnetic field and complete the complete even-odd 22-year cycle. The numerical parameter is proposed that characterizes the GOR efficiency, which increases in the decay phase of SSN cycles. If the GOR is fulfilled, then within the framework of the Leighton model, the Bpol values have a constant contribution of the relic magnetic field < |-10| μT. An algorithm for searching for the beginning of SA cycles (integral maxima/minima) according to SSN, Bpol and NM MOSC data has been developed and applied. The times found do not coincide with each other, and the beginning of cycles according to Bpol always advances, and the greatest delay corresponds to the minimum of 23-24 SSN cycles.

Keywords: *solar activity, even and odd cycles, polar magnetic field, Gnevyshev-Ohl effect, galactic cosmic rays, modulation, relic field*

DOI: 10.31857/S00167940250722e6

1. INTRODUCTION

When carrying out and planning space activities outside the Earth's magnetosphere, it is necessary to know the expected radiation conditions that are created by solar proton events (SPEs) and galactic cosmic rays (GCRs). At the same time, the real radiation hazard is posed by SPEs

whose maximum intensity exceeds the GCR modulation depth in the solar activity (SA) cycle. Spacecraft should be adapted to flights within the limits of possible variations of GCL. Extreme-high (in the pair of 22-23 cycles) and extreme-low (in the pair of 24-25 cycles) levels of SA allow us to test our knowledge of radiative conditions in the heliosphere. For example, in [Belov et al., 2005], a forecast of the GCR intensity in the 24th cycle was made, with the maximum predicted in 2006-2007. The actual maximum was delayed by ~2 years, which was later explained by anomalies of this period [Gushchina et al., 2013].

An analysis of the methods and results of forecasting the 24th and 25th cycles [Nandy, 2021], showed that the forecasts for the 24th-25th cycles based on different methods diverged from each other, but only the forecasts for the 25th solar cycle based on physical models converged, indicating a weak or moderately weak 25th spot cycle. According to Nandy [Nandy, 2021] this unity in predictions is evidence that the Babcock-Leighton mechanism ([Babcock, 1961; Leighton, 1964, 1969]) is the dominant driver of solar cycle variability on decadal time scales, and that the short dynamo memory of the solar dynamo mechanism allows predictions to be made only for the next spot cycle. In 2024, monthly mean SSN values have already repeatedly surpassed the maximum annual mean SSN value of 127 predicted for the current 25th cycle, lying between the SSN maxima of the 20th and 24th cycles [Pal and Nandy, 2024].

The Babcock-Leighton dynamo mechanism (see [Charbonneau, 2020] for a review) represents two processes: one is the annihilation of the leading polarities in the two hemispheres near the equator, the other is the drift and diffusion of the slave polarity to the poles. The unipolar magnetic regions obtained in this way neutralize the poloidal field of the current cycle at the poles (the growth phase of the spot cycle) and generate the poloidal field of the next cycle of the opposite sign (the decline phase of the spot cycle) for the new SA cycle.

According to [Leighton, 1969], the primary quasi-stationary poloidal magnetic field, which should be generated below the convective zone and, accordingly, should not change sign in the cycles, is necessary for the dynamo to start its operation. Apparently, [Piddington, 1976] was the first to consider theoretically the contribution of primary (relic) magnetic fields to CA. Hereinafter, we will refer to a quasi-stationary large-scale magnetic field with a characteristic time of change much longer than 11 years as a relic field. In the English-language literature, in addition to "*relic"* [Bravo&Steart, 1995; Mursula et al., 2001] there are terms *"primordial"* [Piddington, 1976; Pudovkin&Benevolenskaya, 1982] *and "fossil"* [Levy&Boyer, 1982].

The magnetic-hydrodynamo, which generates oscillating magnetic fields in the presence of an external ambient magnetic field, introduces a noticeable asymmetry between the two halves of the full magnetic cycle [Levy&Boyer, 1982], so the asymmetric solar cycle should indicate the presence of a stable dipole moment of the relic magnetic field ("*a fossil magnetic field"*) under the

convective zone of the Sun. Pudovkin and Benevolenskaya [Pudovkin&Benevolenskaya, 1982] related the relic magnetic field of the Sun to the Gnevyshev-Ohl rule (GGO) [Gnevyshev, Ohl, 1948], determined the direction of the relic field and estimated its magnitude from the observed asymmetry of even-odd cycles. According to PGO, the sum of sunspots in the preceding even cycle is smaller than in the subsequent odd cycle.

The authors of [Mursula et al., 2001] have shown the existence of a stable 22-year CA cyclicity over the last 400 years (the time of direct solar observations), and consider it as evidence of a constant (at least on a time scale of several hundred years) relic dipole magnetic field. Nagovitsyn [Nagovitsyn, 2024] concluded that the PGO is valid for the 410-year interval as a whole without excluding the pair of Zurich cycles 4 and 5 adopted in the rule earlier. According to Ishkov [Ishkov, 2022] the PGO was violated the only time in the history of the valid series, when the 22nd (the largest among even cycles) became higher than the 23rd odd cycle.

Tlatov [Tlatov, 2013] believed that the violation of the GWP in the 22nd-23rd cycles could be a sign of a long-term change of the GWP in the next cycles, and suggested the existence of a permanent solar magnetic field that could change polarity, reversing the sequence of 22-year cycles. Tlatov [Tlatov, 2015] found a periodicity with a period of ~200 years and rejected the relict field hypothesis. At the same time, he suggested the presence of a slowly changing magnetic field in the Sun, which affects the amplitude of 11-year CA cycles and predicts the 25th cycle to be weaker than the 24th, if his hypothesis were correct.

The authors of [Cliver et al., 2024] argue for the existence of a small-scale turbulent dynamo on the Sun that is independent of the 11-year cycle. Generated by this unchanging dynamo, the small-scale magnetic fields, maintain a constant open magnetic flux of the solar wind (SW). The observed intensity of GCRs is the result of their modulation by the CB plasma in the large volume of the heliosphere. The GCR flux carries information about the global properties of the heliosphere in different phases of the SA cycles. The GCR variations observed in even and odd cycles indirectly confirm the chaotic Babcock-Leighton SA mechanism [Struminsky et al., 2025]. They do not respond to the chaotic polarity of the heliosphene magnetic field, which is expected during the growth phase and near the maximum (repolarization) of the new solar cycle. However, the decline phase of the cycle shows a clear difference in the GCR variations in even and odd cycles, corresponding to the polarity of the global dipole magnetic field after the repolarization [Struminsky et al., 2025]. The observed asymmetry of activity (visible in Bpol, GCL, and SSN) qualitatively corresponds to the PGO, namely, in odd cycles, sunspots (additional compared to the paired even cycle) can appear during the prolonged phases of activity maximum and decline, which are necessary to fulfill the PGO. At the same time, the relationship between SSN changes and the magnitude of the magnetic flux carried to the poles (increase/decrease of Bpol) is not precisely

known and may be different at different phases of the cycle. This may lead to a failure to fulfill the PGO in its original formulation.

The aim of the paper is to find evidence indicating the existence of a PGO analog in observational GCR data, requiring the sign of the particle charge and the polarity of the magnetic field to be taken into account. The paper also provides an interpretation of this rule from the physical point of view (according to the authors) on SSN observations (as a proxy of magnetic SA). The possibility of relic field traces in the Bpol data is discussed.

2. DATA ANALYSIS: SUNSPOT NUMBERS, POLAR MAGNETIC FIELD AND HCL MODULATION

Here we consider the time scales associated with SA over the full 22-year magnetic cycle, according to the available SSN data (https://www.sidc.be/SILSO/datafiles), GCR fluxes (https://cr0.izmiran.ru/mosc/), and Bpol values (http://wso.stanford.edu/Polar.html). These data are shown in Fig. 1 (top, middle, and bottom panels, respectively), relative to the even-cycle GCR intensity maximum in the even-odd pair (zero on the time scale). For the construction of Fig. 1, we took the GCL maxima from [Struminsky et al., 2025], and the SSN minimum of the 18th cycle for the pair of 18-19 cycles. For reference, the dates of the GCR maxima in odd cycles are given in the legend in the upper panel.

In Fig. 1, two points are noteworthy. First, the different position of even minima of SSN cycles, consistent with the "flat" maxima of the GCR. "Sharp" GKL maxima correspond to SSN minima in odd cycles. This feature (the shape of maxima) of the GCR intensity was observed in the observations of the Climax neutron monitor for the period from 1959 to 1979 and modeled [Jokipii and Thomas,1981]. The manifestation of the PGO analog in the CA-modulated GCR flux is the shape of the GCR intensity maxima "flat maximum" in even cycles and "sharp maximum" in odd cycles. However, their theoretical representations could not explain the transition from "flat" to "sharp" state. Second, we can see that the deepest modulation of the GCL in even cycles was at the SSN growth phase in the 22nd (black curve, middle panel, Fig. 1), and in odd cycles it was at the SSN growth phase in the 23rd (red curve, ibid.). These time periods are known for the 1989-1991 and 2000-2001 super outbreaks. In addition, the SSN and GCR fluctuation amplitudes of other pairs also show interpretable agreement. This makes it possible to estimate in pair 18-19 the level of GCL modulation in pairs 18-19 where their observations are missing.

The shortest Bpol data series (bottom panel, Fig. 1) also shows interpretable agreement with simultaneous SSN and GCL observations. Taking into account the hypothesis of the presence of the Sun's relic magnetic field [Pudovkin & Benevolenskaya, 1982; Levy&Boyer, 1982], the first in the pair of 22-year full magnetic cycles should go even cycle with negative Bpol. The transition of the 22-23 pair (black and red curves, bottom panel, Fig. 1) to the 24-25 pair (blue and green curves,

ibid.) occurs at Bpol values ~ (-50)μTl, which is the minimum magnetic state of the Sun [Cliver, von Stieger, 2017; Schrijver et al., 2011]. During the first 3 years of the pair of 22-23 cycles (black and red curves, bottom panel of Fig. 1), the sign of Bpol corresponds to that of the relic field. Its existence is indicated, for example, by the period of the greatest convergence of the curves (polarity reversal, repolarization) odd cycles 21 and 23 (pink and red curves, bottom panel, Fig. 1), which reveals the addition of some value to the Bpol value, making the final field different from 0.

3. METHODS AND APPROACHES. THE PROBLEM OF SELECTING ZERO IN THE DATA

There are currently ~24.5 cycles of SSN observations over ~400 years (see, for example, the SILSO database (https://www.sidc.be/SILSO/datafiles). There are already ~4.5 cycles of GCR intensity measurements (e.g., NM MOSC) and Bpol values (Wilcox, WSO) that coincide in time, which allows us to consider the modulation problem as a whole against the background of SSN activity.

Since the study of cyclic activity is traditionally based on observations of sunspots and counting their daily number on the visible hemisphere of the Sun, the date when there are no sunspots on the disk or with the smallest number of sunspots (the minimum found in this way) is taken as the beginning of the cycle. We used this to construct the pair 18-19 (Fig. 1, upper panel) because of the absence of GCR observations in the 18- cycle. This approach is good for analyzing and forecasting based on statistics. Our idea is to use as 0 the beginning of the observation of physical processes (e.g., electromagnetic radiation registration at microwaves or in X-rays) to study specific events [Struminsky et al. 2020]. In this work, we take periods (as described above) as the beginning of the time scale in observations related to long-lasting physical processes, i.e., slowly changing SA characteristics - GCL modulation or Bpol course - as the beginning of the time scale.

Let us describe our method for determining the maxima. Let *f(t)* be a time series with some number of "humps" and "troughs". "Hump" series *f(t)* is a "hump" series *-f(t)*, hence we consider only "humps" in the following. If between the leading and trailing edge of a "hump" (i.e., in the maximum phase) of *f(t*) its deterministic component varies weakly, then the moment of time at which the actual local maximum within a single "hump" is reached is obviously random: it can vary very widely in the same situations. Therefore, we want to have a tool for finding the entire set of local maxima *f(t)* that takes into account the meaningful "humps" in their entirety, i.e., their rise, maximum, and fall phases, and also ignores the non-meaningful "humps". For this purpose, we introduce a new function $I(t)$, having time dimension, and consider its local maxima. The function *I(t)* is related to the original time series *f(t)* through a single parameter (t) , which depends on time *t* and is defined as the weighted average of the moments of time inside the "right horizon":

$$\langle t \rangle = \frac{\sum_{t \le \xi \le \beta(t)} \xi \left(f(\xi) - f(t) \right)}{\sum_{t \le \xi \le \beta(t)} \left(f(\xi) - f(t) \right)} \quad . \tag{1}$$

Formula (1) summarizes the parameter ξ , the "right horizon "ξ is equal to

$$\beta(t) = \arg \min_{\substack{f(\xi) < f(t) \\ \xi > t}} \xi \quad . \tag{2}$$

This is the closest point ξ to the right of *t,* in which *f*(ξ) becomes smaller than *f*(t) (the graph of the function dives as if under the horizon, hence the name).

The function *I(t)* is defined as the sum of Gaussian exponentials, each centered at a different point (t) , over all samples of the original time series *f(t)*:

$$I(t) = 2 \langle \delta t \rangle \sum_{\forall t} \exp\left(-\left(\frac{t - \langle t \rangle}{\langle \delta t \rangle} \right)^2 \right) \quad . \tag{3}$$

Here $\langle \delta t \rangle$ denotes the average time between time series samples. When *t* gets to the rising phase of the "hump", $\langle t \rangle$ falls into its "visual middle" (taking into account the geometry of its fronts) and actually stops changing. The component of the sum in formula (3) corresponding to the phase of ascent contains Gaussian exponentials centered approximately at one point, and there are more such exponentials the more extended in time the "hump" is. We have chosen the coefficient in front of the sum (3) in such a way that the value of the local maximum of the function *I(t*) is approximately equal to the time extent of the "hump" within which this local maximum is located.

Thus, *I(t)* is almost everywhere equal to zero and has sharp (width of the order of tens $\langle \delta t \rangle$) peaks, the tops of which are located at the points of "visual maxima" of the "humps", and the height of these peaks is approximately equal to the duration of each "hump". We ignore local "roughnesses of relief" of the *f(t)* function if their duration is less than the characteristic time of significant changes in the solar activity trend, i.e., *T = 1000* days. Thus, we call integral maxima of order *T* the set of local maxima of the function *I(t)* on the intervals where $I(t) > T$. Integral minima are obtained by replacing the time series $f(t)$ by the series $-f(t)$.

The time course of the Bpole data is plotted in Fig. 2; the vertical straight lines show the Bpole maxima, NM MOSC counts, and SSN minima we found in the cycles, which are summarized in Table. The delay times of the integral maxima of GCLs and integral SSN minima relative to the integral maxima of |Bpol| (see Fig. 2) are summarized in Table. Here and hereafter we refer to the integral maxima and minima. In all cases presented in the Table (except for minima 20-21), the maximum of the GCR intensity relative to the SSN minimum is expectedly delayed from 5 to 9

months, which approximately corresponds to the time of SSN propagation from the Sun to the heliospheric boundaries. The lag of the GCR intensity relative to |Bpol| varies from 1 year to 3 years, which phenomenologically corresponds to the course of SSN minima relative to |Bpol| maxima. The lag of SSN minima relative to |Bpol| maxima shows that the formation of the solar dipole occurs earlier than the end of spot activity. The available data show that the |Bpol| maximum occurs earliest. The physical process responsible for |Bpol| works out its scenario earlier than the mid-scale magnetic field (whose proxy is SSNs) and GCR modulation. The advance of the SSN minima relative to the maxima of GCL indicates the contribution to the GCL modulation of the strong spot magnetic field in addition to the influence of Bpol.

In minima 20-21, on the contrary, the maximum of the GCL intensity is ahead of the SSN minimum by about 7 months. This behavior of GCL is possibly related to the drift mechanism of GCL propagation, since at this time the field in the heliosphere was positive and the drift worked against convection [Jokippi et al., 1977]. The Sun's dipole magnetic field (Bpol) can be considered as a proxy of the magnetic field in the heliosphere at the SSN decline [Struminsky et al., 2025]. The Bpol maximum should always precede the SSN minimum, so the GCR maximum in the 20-21 minimum, obtained with a noticeable drift contribution, can precede the SSN minimum and indirectly indicate the necessary value of Bpol. It should have been larger in the 20-21 cycle minimum than in the 22-23 minimum (see the reasoning in Section 5. Discussion). It is possible that in the 22-23 minimum, the GCR intensity maximum could also be ahead of the SSN minimum if there was no deepest GCR minimum in 1991.

4. INTERPRETATION OF THE GNEVYSHEV-OHL RULE

The Gnevyshev-Ol rule (GGO) reveals asymmetry both within the even-odd ((2n)-(2n+1)) pair of cycles and in the intersection of ((2n-1)-(2n)-(2n+1) pairs - the preceding even with odd and odd with the following even, which corresponds to the negative polarity of the relic magnetic field. If we talk about the full 22-year magnetic cycle, which begins with the 11-year (2n) cycle and ends with the 11-year (2n+1) cycle, we should keep in mind that it obviously involves the magnetic fields of both the previous (2n-1) and subsequent ((2n+1)+1) cycles. "Magnetic memory" realized in magnetic structures, whose proxy carriers I mi are sunspots. Information about (2n-1) cycle is "erased" during the repolarization of (2n) cycle, and "magnetic memory" about (2n) cycle is "erased" during the repolarization of (2n+1) cycle. Thus, ((2n+1)+1) knows nothing about its predecessors except the value of Bpol stored in the decline phase of the (2n+1) cycle. That is why the most reliable predictions of the value of the next SSN maximum can be given at the decline phase of the previous cycle 3 years before its minimum (the moment when Bpol formation for the next cycle ends [Iijima et al., 2017; Kumar et al., 2021; Nagovitsym&Ivanov, 2023]).

The SSN cycle maximum represents a period of "quasi-equilibrium", when there are no

longer any remnants of the magnetic field of the previous solar cycle at the poles (zero magnetic moment of the polar dipole - repolarization), and the magnetic field of the subsequent cycle is still insufficient for the transition to the formation of the field of the new cycle. By "quasi-equilibrium" we mean the interaction of a large number of spots of different polarity, which corresponds to a zero magnetic flux drifting from the equator to the poles. In the "magnetic memory" of a cycle, not the maximum SSNs and not their sum over the cycle are stored, but only the maximum dipole moment Bpol, which allowed the available sunspots to form.

In some cycles two SSN maxima are seen, the first of which corresponds to the number of sunspots, which is necessary for the final destruction of the old field, and the second - for the transition from the state of quasi-equilibrium to the construction of a new field of a different polarity. When the duration of repolarization is small, merging of maxima is possible; such cycles have a single maximum. According to the review [Petrovay, 2020] the best methods for predicting CA were those based on Bpol observations. These methods can make an estimate of the minimum value of the first maximum of the SSN cycle, but the maximum value of the SSN cycle seems to be determined during the repolarization (before the Bpol of the new polarity starts to grow). The second maximum can be either larger or smaller than the first.

Let us illustrate our interpretation of PGO and introduce the notion of direct residual efficiency of PGO. Let A^i_{even}, B^i_{even} denote, respectively, the beginning and end of even cycle number *i*, and A^i_{odd}, B^i_{odd} denote the beginning and end of odd cycle. Let us define the direct residual CSGO efficiency *E(t)* as a function of the distance *t* from the beginning of the cycle as:

$$E(t) = \underset{i=1,2,\ldots}{median}\left(\frac{\sum_{A^i_{odd}+t\le\eta\le B^i_{odd}} SSN(\eta) - \sum_{A^i_{even}+t\le\eta\le B^i_{even}} SSN(\eta)}{\sum_{A^i_{even}+t\le\eta\le B^i_{even}} SSN(\eta)} \right) \quad (4)$$

Here, the operator *median* means calculating the median by the indices *i* - pair number, and the summation is done by the variable η - the current time in the solar cycle interval. Hereafter, for brevity, we refer to the distance *t* from the beginning of the cycle as the "cutoff".

In Fig. 3a we plot the time course of the calculated "residual" direct efficiency of the CCP, which is compared with SSN observations in cycles 18-23. In calculating the direct efficiency, pairs of cycles starting from cycle 8 were taken due to the incompleteness of cycle 6 at the SILSO site.

In the plot of the direct efficiency of the CCP, we note that as a function of the "cutoff" the efficiency value decreases slightly for the "residuals" after ~4.2 and ~5.6 years from the beginning of the cycle, and then begins to rise sharply upward after ~7.3 years. Note that the direct efficiency of the CSG at zero cutoff (native CSG) of 20% is not much larger than the characteristic relative error in the SSN of 11%. Switching from native CSG to residuals-based CSG increases this gap

many times over. The efficiency of PGO by "residuals" rises sharply to tens of percent at *t* after the second bifurcation point (see discussion below), which is already several times larger than the characteristic relative error of SSN.

We also performed an experiment with the reverse ordering of cycles in pairs and computed the inverse efficiency of the PGO:

$$E_{inv}(t) = \underset{i=1,2,\ldots}{median}\left(\frac{\sum_{A^i_{even}+t\le\eta\le B^i_{even}} SSN(\eta) - \sum_{A^i_{odd}+t\le\eta\le B^i_{odd}} SSN(\eta)}{\sum_{A^i_{odd}+t\le\eta\le B^i_{odd}} SSN(\eta)}\right). \quad (5)$$

When calculating the inverse efficiency of PGO, pairs of cycles starting from the 7th cycle were taken. In Fig. 3b plots the inverse efficiency of PGO, in which we note three features. First, the inverse CSI efficiency is negative at all "cutoffs", i.e., the CSI efficiency is an antisymmetric function with respect to even-odd permutations and shows the asymmetry of even-odd cycles. Second, it is modulo comparable to the direct CSG efficiency for about the first 5 years (the first ~3 years is (-10%), comparable to the SSN error, and the section from ~2.9 to ~5.3 years with an efficiency of (-20%) is clearly visible). Third, further, the inverse efficiency of the PGO barely reaches (-30%), and its monotonic decline is interrupted.

Recall that the PGO is a consequence of magnetic field generation by the Babcock-Leighton mechanism, in the presence of an already existing field. The solar cycle model [Leighton, 1969] was modified in [Pudovkin&Benevolenskaya, 1982], where the authors assumed that there exists a *primordial* (*primordial*) and *nondecaying* (*nondecaying*) poloidal magnetic field. According to the estimates [Pudovkin&Benevolenskaya, 1982], the polarity of the primordial magnetic field should be negative, and its magnitude is ~0.5 Gs (50 μTL), which surprisingly coincides with the magnitude of the polar magnetic field measured at the minimum of 23-24 SSN cycles (2008-2009), when the Sun was in its minimum magnetic state [Schijver et al., 2011; Cliver&von Steiger, 2017].

Note that according to the ideas of Mordvinov and Kitchatinov [Mordvinov& Kitchatinov, 2004], the contribution of large-scale magnetic structures to the total signal does not exceed 20 μTL, and the contribution of the relic magnetic field does not exceed 8 μTL in amplitude. Also an argument against the relic field value of (-50) μTL is the almost mirror symmetry with respect to the straight 0 μTL Bpole curves in the 24th and 25th cycles *before the* repolarization and in the 23rd and 24th cycles *after* it (see the left panel in Fig. 3, [Struminsky et al., 2025]). Apparently, the magnitude of the relic field should be less than |-10| μTl. The non-symmetry of even and odd SSN cycles (classical PGO) means that the current "magnetic memory" is erased during repolarization, but the "magnetic memory" of the relic field always remains.

In [Struminsky et al., 2025], it was suggested that there are two bifurcation points in the time dependences of Bpol odd cycles, located, respectively, ~5.5 years and ~7.5 years after the GCR maximum. These points determine the scenario of further development of the cycle - polar field

accretion. At the first point (~5.5 years) there is a choice between scenarios leading to super-strong (stronger than 22nd) or strong (22nd) cycles, and at the second point (~7.5 years) - between scenarios leading to strong (22nd) or weak (24th) cycles (see above description of Fig. 1). The direct GWP efficiency (Fig. 3a) calculated from SSN data shows features at the ~4.2, ~5.6, and ~7.3 year cutoffs, while the plot of the inverse GWP efficiency (Fig. 3b) highlights the period from ~2.9 to ~5.3 years. These characteristic time points appear to indicate the asymmetry of SSN activity. In even cycles in the period from ~2.9 to ~5.3 years, there is a state of dynamic equilibrium - the field workup (repolarization) and, further, there is an active Bpol workup up to ~7.3 years. In odd cycles, the state of dynamic equilibrium from ~4.2 to ~5.6 years is observed and, further, there is an active development of Bpol of new polarity up to ~7 years and more. Sunspots formed during the period of dynamical equilibrium do not contribute to the dipole moment of the new cycle and should not be taken into account in its prediction.

5. DISCUSSION

The authors of [Iijima et al., 2017] draw attention to the plateau of the dipole moment observed ~3 years before the minimum and show that the magnetic flux transport across the equator is close to 0 at this time. Emerging new sunspots do not contribute to the axial dipole moment. According to the authors of [Kumar et al., 2021], available observations and models indicate that the earliest time that can be safely used as a precursor to Bpol is 4 years after the Bpol sign change, which typically occurs 2-3 years before solar minimum and ~7 years before the predicted maximum. Nagovitsyn & Ivanov [Nagovitsyn&Ivanov, 2023], actually repeated these conclusions, but without mentioning the Bpol dynamics, proposing to use the index of the third year before the minimum [SNm-3] in the descending phase of the previous odd cycle as a precursor of the subsequent even cycle, and to predict the odd cycle amplitude - the 7th year before its maximum [SNM-7] in the descending phase of the previous even cycle.

On the other hand, the only clear violation of PGO [Ishkov, 2022] in the history of a reliable SSN series in the 22-23 pair could hardly be predicted from the dipole moment plateau ideas, since the dipole moment plateau was not observed in cycle 22. Indeed, the maximum Bpol level in 1992 was ~106 μTL (~104 μTL in the integral Bpol maximum in December 1994), but the Bpol level dropped to ~96 μTL by the SSN minimum in 1996. It can be assumed that the result of sunspots in 1994-1996 was the accretion of a negative magnetic flux that reduced the Bpol value within 2 years to the SSN minimum. Eventually the work of cycle 23 was done by cycle 22, which allowed cycle 23 to be the weaker of the pair.

The question arises as to the premise behind the choice of a particular scenario (is it spontaneous or deterministic)? According to the study [Jiang et al., 2015] the reason for the weak polar field at the minimum of cycles 23-24 and, consequently, for the weak cycle 24, was large

bipolar regions that appeared at low latitudes with the "wrong" (opposite to most regions) orientation in the north-south direction. The authors of [Kumar et al., 2024] managed to model different scenarios of polar field accumulation by changing the characteristics of the bipolar regions. According to the authors of [Pipin et al, 2023], *the data driven models* show that the weak 24th cycle cannot be explained using only the properties of bipolar magnetic regions. This weak cycle and the long SA minimum preceding it were probably caused by a decrease in turbulent *helicity in the bulk of the convection zone* during the garden phase of cycle 23.

In our opinion, the spots in the maximum of the 25th cycle can be not much more than 200, and it will be passed after the transition of Bpol value (-50 μTL), probably in 2027. And the next 22-year CA cycle will start in 2031-2032. Also, the possible failure to take into account the relic magnetic field in modeling the solar dipole moment in [Pal and Nandy, 2024] made the 19th cycle a notable exception to the cycles they considered. In addition, the calculated dipole moment in cycle 19 differed significantly from that estimated from observations, which made the reconstruction of cycle 20 impossible.

On the basis of our ideas about the connection of GCL modulation with the change of Bpol and SSN , as well as the connection of Bpol and SSN among themselves [Struminsky et al., 2025], let us present mentally a possible course of the Bpol curve of the 20th cycle according to SSN observations and GCL modulation. In the bottom panel of Fig. 1, the *conceivable yellow curve* of cycle 20 should lie between the black and blue curves of cycles 22 and 24 until year 3, so that the SSN maximum of cycle 20 was larger than cycle 24 but smaller than cycle 22. *It* should then follow the blue curve of cycle 24 until year 7, since from year 3 to year 7 the modulation of the GCR in cycle 20 was the same as in cycle 24. After year 7, the *mental yellow curve* should become just above the black and red curves (cycle 22-23 pair) and join the pink curve of cycle 21, since the number of spots during this period of cycle 20 was higher and the modulation of GCL was almost the same, compared to the same period of cycle 22-23 pair. It is possible that from years 8 to 11 of cycle 20, the generation of spots was not accompanied by a transfer of new magnetic flux towards the poles (see ideas in [Iijima, et al., 2017]), which could have provided a constant polar field at the level of the first Bpol observations (pink curve). Unfortunately, we cannot repeat the same reasoning for the 18-19 pair due to the lack of GCR data. However, we can argue that the magnitude of Bpol in cycle 18 should be the maximum observed [Pal and Nandy, 2024] to make a large SSN cycle 19.

6. CONCLUSIONS

– The Gnevyshev-Ol rule is a consequence of magnetic field generation by the Babcock-Leighton mechanism in the presence of a relic field. When interpreting the PGO, the SSN sum should be considered as the total magnetic flux transported to the polar regions over the SA cycle,

which should be smaller in even cycle than in the next odd cycle.

– Polar magnetic field measurements always contain a relic field contribution. The almost mirror symmetry, relative to the "repolarization" (0 μTl), of the Bpol curves in the 24th and 25th cycles *before* and in the 23rd and 24th cycles *after* it indicates that the magnitude of the relic field is less than |-10| μTl.

– In even-odd pairs, the Gnevyshev-Ol rule is more pronounced (the efficiency of the PGO increases) at the phases of polar field development (at the decline phases of SSN cycles).

– The non-fulfillment of the Gnevyshev-Ol rule in the pair of 22-23 cycles is apparently due to spots (connected active regions) in the growth phase and in the maximum of cycle 22, which did not contribute to Bpol. Perhaps in the SSN maximum of cycle 19 the spots gave a disproportionately small contribution to Bpol.

– A manifestation of the PGO analog in the SA-modulated GCR flux is the shape of the GCR intensity maxima: a "flat" maximum in even and a "sharp" maximum in odd cycles.

ACKNOWLEDGEMENTS

The authors thank the participants of the observations and the creators of the databases (http://wso.stanford.edu/Polar.html and https://www.sidc.be/SILSO/datafiles), which were used in this work, for the invested labor and the possibility of open access to the data. The authors are grateful to the teams of the CL World Network of stations and the NMDB project (https://www.nmdb.eu/).

The authors would like to thank their colleagues without whom this work would not have been possible: Yu.A. Nagovitsyn, N.G. Makarenko, V.N. Obridko, M.L. Demidov, V.I. Abramenko, A.M. Sadovsky, A.V. Belov, R.T. Gushchina, and V.G. Yanke.

FUNDING

This work was supported by subsidies under the topics "Plasma" at IKI RAS and "Multi-wavelength active Sun: a comprehensive analysis" at GAO RAS.

CONFLICT OF INTERESTS

The authors declare that they have no conflict of interest.

REFERENCES

1. *Belov A.V., Gushchina R.T., Obridko V.N., Shelting B.D., Yanke V.G.* Forecast and epignosis of long-period cosmic ray variations based on various solar activity indices // Izv. RAS, ser. phys. V. 69. No. 6. P. 890-892. 2005.
2. *Gnevyshev M.H., Ol A.I.* About the 22-year cycle of solar activity. // Astron. zh. 1948. V. 25, No. 1, P. 18-20.
3. *Gushchina R.T., Belov A.V., Yanke V.G.* Spectrum of long-period variations in the minimum

of solar activity in 2009 // Izv. RAS, ser. fiz. V. 77. № 5. P. 577-580. 2013. doi: 10.7868/S0367676513050244

4. *Ishkov V.N.* Results and lessons of the 24 cycle – the first cycle of the second epoch of reduced solar activity // Astron. Zh. 2022. V. 99. No. 1. P. 54-69. doi: 10.31857/S0004629922020050
5. *Struminsky A.B., A.V. Belov, R.T. Guschina, V.G. Yanke, I.Yu. Grigorieva,* On the prediction of galactic cosmic ray modulation in the 25th solar activity cycle // Geomagnetism and Aeronomy. — 2025 in print
6. *Babcock H.W.* The topology of the Sun's magnetic field and the 22-year cycle //Astropys. J. V. 133. P. 572. 1961. doi: 10.1086/147060
7. *Bravo, S. and Stewart, G.* The Inclination of the Heliomagnetic Equator and the Presence of an Inclined Relic Field in te Sun // Astrophys. J. 1995. V. 446. P. 431.
8. *Charbonneau P.* Dynamo models of the solar cycle // Living Reviews in Solar Physics. V. 17. Iss. 4. 2020. doi: 10.1007/s41116-020-00025-6
9. *Cliver E.W. and von Steiger R.* Minimal Magnetic States of the Sun and the Solar Wind: Implications for the Origin of the Slow Solar Wind // Space Sci Rev. 2017. V. 210. P. 227–247. doi: 10.1007/s11214-015-0224-1
10. *Cliver E.W., White S.M., and Richardson I.G.,* A Floor in the Sun's Photospheric Magnetic Field: Implications for an Independent Small-scale Dynamo // Astrophys. J. Let. 2024. V. 961. L46 (7pp). doi:10.3847/2041-8213/ad192e
11. *Iijima H., Hotta H., Imada S., Kusano K., and Shiota D.* Improvement of solar-cycle prediction: Plateau of solar axial dipole moment // A&A 607, L2 (2017). doi: 10.1051/0004-6361/201731813
12. *Jiang J., Cameron R. H., and Schüssler M.* The cause of the weak solar cycle 24 // Astrophys. J. Let. 2015. V. 820. P. L28-L34. doi: 10.1088/2041-8205/808/1/L28
13. *Kumar P., Karak B. B. and Sreedevi A.* Variabilities in the polar field and solar cycle due to irregular properties of bipolar magnetic regions // MNRAS. 2024. V. 530. P. 2895–2905. doi: 10.1093/mnras/stae1052
14. *Leighton R.B.* Transport of magnetic fields on the Sun // Astrophys. J. V. 140. P. 1547–1562. 1964. doi: 10.1086/148058
15. *Leighton R.B.* A magneto-kinematic model of the solar cycle // Astrophys. J. 1969. V. 156. P.1–26. doi: 10.1086/149943
16. *Levy E.H. and Boyer D.* Oscillating Dynamo in the Presence of a Fossil Magnetic Field. The Solar Cycle // Astrophys. J. 1982. V. 254. P. L19-L22.1
17. *Mordvinov, A.V. and Kitchatinov, L.L.* Active Longitudes and North-South Asymmetry of the

Activity the Sun as Manifestations of Its Relic Magnetic Field // Astron. Rep. 2004. V. 48. No 3. P.254-260. doi:10.1134/1.1687019

18. *Mursula K., Usoskin I.G. and Kovaltsov G.A.* Persistent 22-year Cycle in Sunspot Activity: Evidence for a Relic Solar Magnetic Field // Sol. Phys. 2001. V. 198. P. 51–56.
19. *Nagovitsyn Yu.A.* Confirmation of the “Lost” Cycle and the Gnevyshev–Ohl Rule in a Series of Sunspot Areas Spanning 410 Years // Astron. Let. 2024. V. 50. No. 8. P. 529–535. doi: 10.1134/S1063773724700397
20. *Nagovitsyn Y.A. and Ivanov V.G.* Solar Cycle Pairing and Prediction of Cycle 25 // Sol. Phys. 2023. V. 298. P. 37. doi:10.1007/s11207-023-02121-w
21. *Nandy D.* Progress in Solar Cycle Predictions: Sunspot Cycles 24–25 in Perspective // Sol. Phys. 2021. V. 296. P. 54. doi: 10.1007/s11207-021-01797-2
22. *Pal S. and Nandy D.* Algebraic quantification of the contribution of active regions to the Sun’s dipole moment: applications to century-scale polar field estimates and solar cycle forecasting // MNRAS. V. 531. P. 1546–1553. 2024. doi: 10.1093/mnras/stae1205
23. *Petrovay K.* Solar cycle prediction. Living Rev. Sol. Phys. V. 17: 2. 2020. doi: 10.1007/s41116-020-0022-z
24. *Piddington J.H.,* Solar manetic field and convection: the primordial field theory // in Basic Mechanism of Solar Activity IAU Sympos. No 71. Reidel 1976. PP. 389-407.
25. *Pipin V.V., Kosovichev A.G., and Tomin V.E.* Effects of Emerging Bipolar Magnetic Regions in Mean-field Dynamo Model of Solar Cycles 23 and 24 // Astrophys. J. V. 949. P. 7 (13pp). doi:10.3847/1538-4357/acaf69
26. *Pudovkin M.I. and Benevolenskaya E.E.,* The Qyasisteady Primordial Magnetic Field of the Sun, and the Intensity Variations of the Solar Cycle // Sov. Astron. Let. 1982. V. 8. No. 4. P. 273-274
27. *Schrijver C.J., Livingston W.C., Woods T.N., and Mewaldt R.A.* The minimal solar activity in 2008–2009 and its implications for long-term climate modeling // Geophys. Res. Let. 2011. V. 38. L06701. doi:10.1029/2011GL046658
28. *Tlatov A.G.* Reversals of Gnevyshev-Ohl Rule // Astrophys. J. Let. V. 72. L30 (4pp). doi:10.1088/2041-8205/772/2/L30
29. *Tlatov A.G. The change of the solar cyclicity mode* // JASR. 2015. V. 55. PP. 851–85. doi:10.1016/j.asr.2014.06.024

Table. Delay times of GCL integral maxima and SSN integral minima relative to |Bpol| integral maxima (shown in Fig. 2).

Bpole IntegralMax - integral maxima with respect to Bpol

NM IntegralMax - the same for GKL

true NM Max - true maxima by GKL

SSN IntegralMin - integral minima by spots

true SSN Min - limits of cycles according to English-language Wikipedia

Min Cycles	**NM IntegralMax**	**SSN IntegralMin**	Δ SSN NM	**Bpol IntegralMax**	Δ Bpol NM	Δ Bpol SSN
19-20	1965.25	1964.58	8		-	-
20-21	1975.25	1975.83	-7		-	-
21-22	1986.83	1986.17	8	1985.83	12	3
22-23	1996.67	1996.25	5	1995.00	20	15
23-24	2009.33	2008.58	9	2006.25	37	28
24-25	2019.92	2019.25	8	2018.92	12	4

FIGURE CAPTIONS

Fig. 1. Solar activity from cycle 18 to the current moment of cycle 25 (green circle) represented by pairs of even-odd cycles (vertical dashed line is the date of the first observations). Full 22-year magnetic cycles annual mean spot numbers - smoothed moving average of SSNv2.0 data (upper panel). GCR flux dynamics - monthly mean NM MOSC counts (middle panel). Polar magnetic field course - filtered averages of Bpol WSO (bottom panel). On the horizontal axis 0 - maxima of the GCR fluxes in even cycles from [Struminsky et al., 2025]; in the 18th cycle, the beginning of the SSN cycle is taken as 0. The colors of the curves correspond to the cycle numbers indicated in the legend.

Fig. 2. Dynamics of the polar magnetic field (Bpol, WSO) since the beginning of observations. Vertical lines are the beginnings of 11-year cycles found by the original algorithm through the determination of integral maxima/minima of the used data: Bpol, SSN and GCR (solid, dashed and dotted lines, respectively).

Fig. 3a. Retrospective of even-odd SSN cycles on an 11-year time scale from the 8th to the 23rd inclusive, curves of annual average spot numbers smoothed by a moving average (right vertical scale, SSNv2.0 data): black - even, green - odd cycles and direct efficiency of the CCP, left vertical scale in % ratio of even- odd SSN values on the "residuals" of the cycles (purple curve). Horizontal scale is years from 0, found by the original algorithm from integral SSN maxima.

Fig. 3b. Similar to Fig. 3a, but shows the inverse efficiency of the PGO (left vertical scale in % ratio of SSN odd-even values on the "residuals" of cycles).

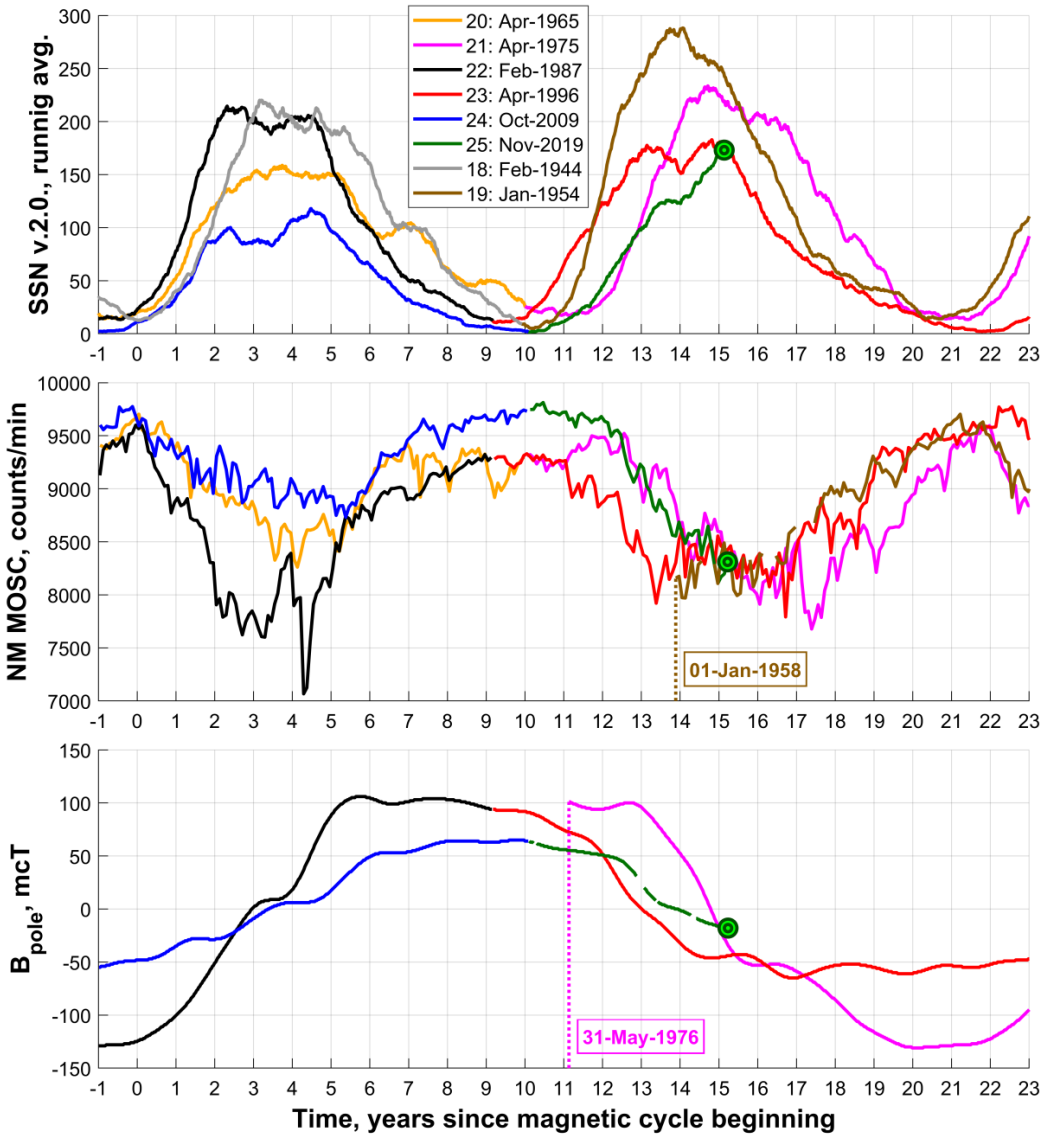
20: Apr-1965
21: Apr-1975
22: Feb-1987
23: Apr-1996
24: Oct-2009
25: Nov-2019
18: Feb-1944
19: Jan-1954
SSN v.2.0., runnig avg.
NM MOSC, counts/min
01-Jan-1958
B pole, mcT
31-May-1976
Time, years since magnetic cycle beginning

Fig. 1.

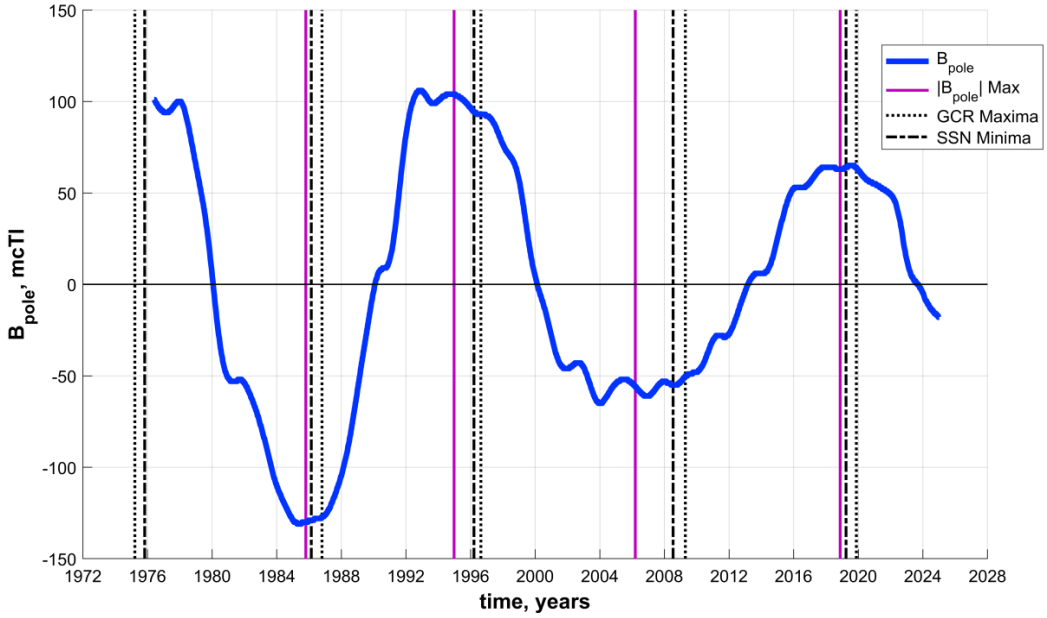
150
100
50
0
-50
-100
-150
1972
1976
1980
1984
1988
1992
1996
2000
2004
2008
2012
2016
2020
2024
2028
B_pole, mcTl
time, years
B_pole
|B_pole| Max
GCR Maxima
SSN Minima

Fig. 2.

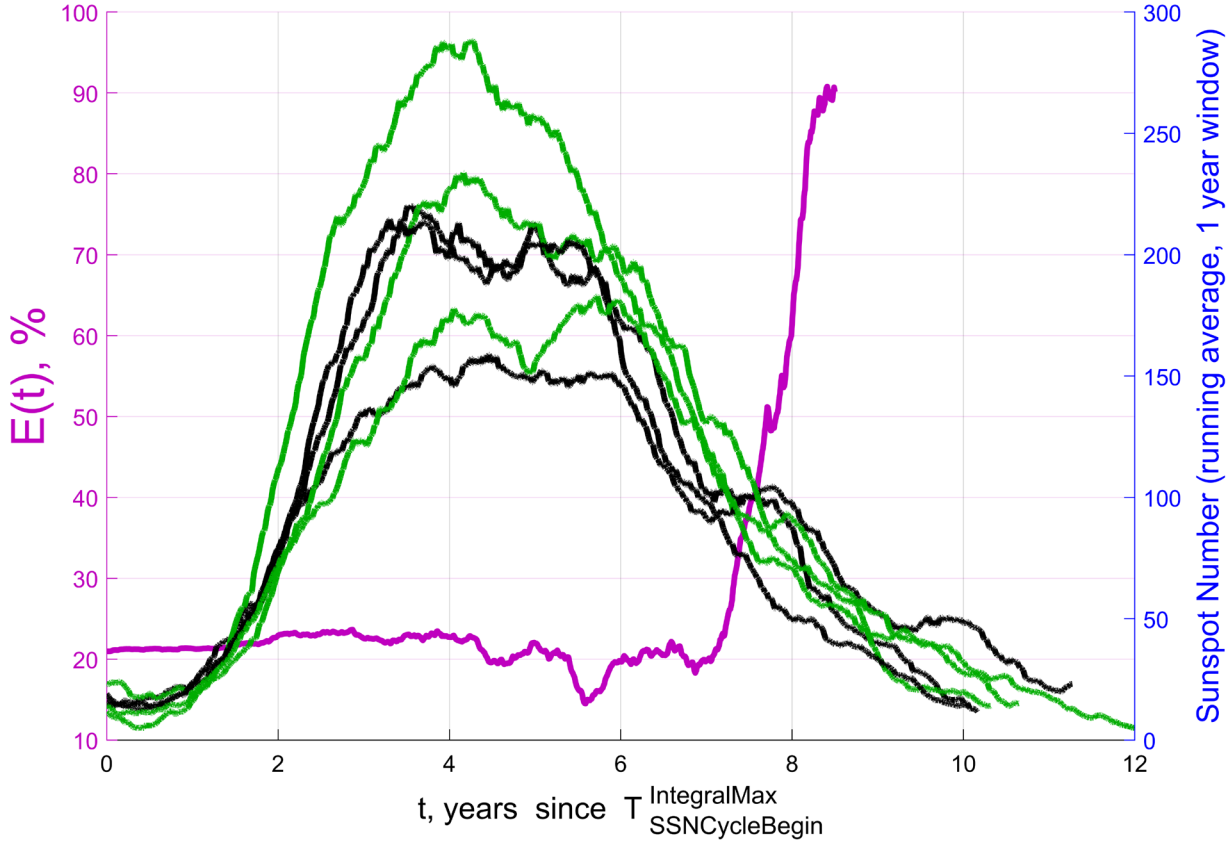
E(t), %
Sunspot Number (running average, 1 year window)
t, years since T IntegralMax SSNCycleBegin
100
90
80
70
60
50
40
30
20
10
300
250
200
150
100
50
0
0
2
4
6
8
10
12

Fig. 3a.

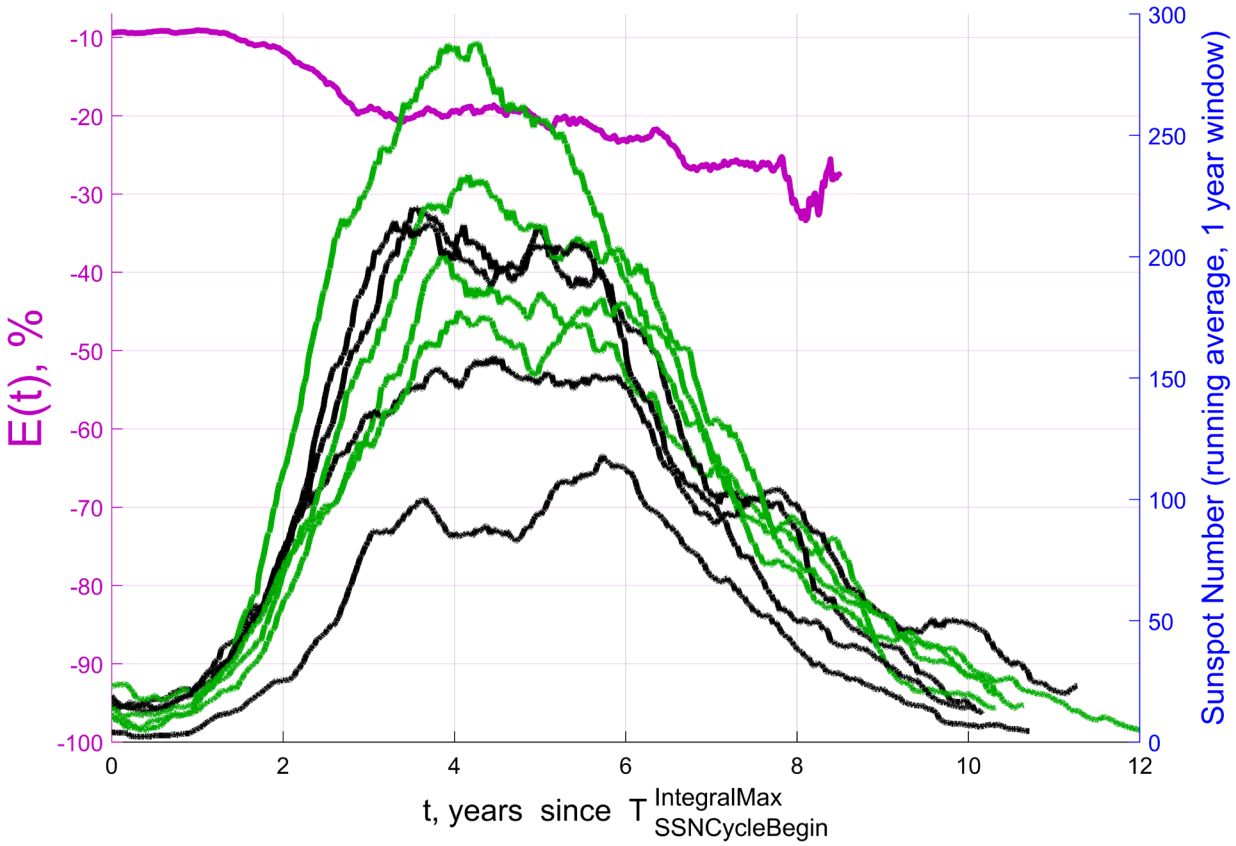
E(t), %
Sunspot Number (running average, 1 year window)
t, years since T IntegralMax SSNCycleBegin
-10
-20
-30
-40
-50
-60
-70
-80
-90
-100
300
250
200
150
100
50
0
0
2
4
6
8
10
12

Fig. 3b.